JOURNAL OF CATALYSIS 79, 420–430 (1983)

Surface Reactions on Rare Earth Metals Monitored by Work Function Measurements

G. STRASSER, E. BERTEL, AND F. P. NETZER

Institut für Physikalische Chemie, Universität Innsbruck, A-6020 Innsbruck, Austria

Received April 28, 1982; revised October 12, 1982

Surface reactions on clean, oxidized, and partially hydrided rare earth metal films with O_2, H_2, H_2O, CO, and CO_2 were monitored by dynamic work function measurements under ultrahigh vacuum conditions. The work function data are discussed in the light of electron spectroscopic evidence, where available. The main results of this study are: Initial oxidation of Yb seems to follow a different oxidation mechanism as compared to other rare earth metals. Reaction of H_2O with clean, oxidized, and hydrided rare earth metal surfaces yields surface hydroxyl species. H_2 uptake on divalent Yb metal is much slower than on trivalent Er metal, but occurs at a comparable rate on the oxidized systems. On oxidized surfaces, surface OH formation is substantiated for room-temperature reaction with H_2. The $\Delta\phi$ data indicate high reactivity of CO and CO_2 toward clean rare earth metal surfaces and are consistent with dissociative adsorption of both molecules.

1. INTRODUCTION

In recent years rare earth materials have attracted growing interest in the surface science community for a number of reasons. For example, rare earths and some of their alloys have been shown to absorb large amounts of hydrogen under suitable reaction conditions. They may be regarded, therefore, as promising candidates for hydrogen storage devices. On the other hand, rare earth compounds are catalytically active in a large variety of reactions, such as oxidation of CO and hydrocarbons, hydrogenation of olefins, olefin isomerization, dehydration of alcohols, etc. Catalytic activities of rare earth compounds have been reviewed by Rosynek (*1*) and more recently by Netzer and Bertel (*2*).

Most of the investigations concerning rare earth catalysis have been carried out under experimental conditions similar to those in practical catalysis. Therefore, impurities were usually not strictly controlled and the catalytically active surfaces were not well characterized. The present study was undertaken to reinvestigate some results of earlier investigations of rare earth catalysis under well-defined reaction conditions. Sample preparation and surface reactions were performed in ultrahigh vacuum, the surface composition was controlled by Auger spectroscopy, and the reactions were monitored by dynamic work function measurements.

The interaction of several gases with rare earth surfaces was studied by electron spectroscopic techniques. Where available, work function data will be correlated with electron spectroscopic evidence. We will then show that, having established basic correlations, quite specific information concerning reactions on various rare earth surface systems can be obtained from dynamic work function measurements. As work function changes were measured with a vibrating Kelvin probe, disturbance of surfaces under investigation is avoided, in contrast to most other surface techniques.

2. EXPERIMENTAL

Experiments were carried out in a stainless-steel UHV system with base pressure $<10^{-10}$ Torr, equipped with the usual facilities for pumping, sample handling, and preparation. Details of the system have been reported elsewhere (*3*). Rare earth metal films were produced by evaporation

0021-9517/83/020420-11$03.00/0

from a tungsten coil onto clean Mo substrates. Surface cleanliness was monitored by Auger spectroscopy and the cleanliness of reactant gases was checked with a quadrupole mass spectrometer.

The work function changes were measured at room temperature with a vibrating Kelvin probe similar to that described by Engelhardt *et al.* (*4*). A tin oxide-coated stainless-steel net served as the reference electrode. The signal produced in the vibrating capacitor was fed into a self-compensating circuit; the changes in compensation voltage are equal to the work function changes and were recorded during the reactions.

3. RESULTS AND DISCUSSION

3.1. Reactions on Rare Earth Metal Surfaces

In order to establish correlations between work function changes and specific surface reactions, interactions of clean rare earth metal films with various gases, which have already been characterized by electron spectroscopy, were investigated first in this study.

3.1.1. Oxidation of rare earth metals by oxygen. In the top panels of Fig. 1 the results of dynamic work function measurements during reaction of Er and Yb metal films with oxygen in the pressure range from $5 \cdot 10^{-9}$ to 3.10^{-7} Torr are displayed. In Er the work function initially decreases to a minimum value, which is apparently pressure dependent. The work function then increases and reaches saturation only after high exposures. The results at low exposures are similar to those obtained by Müller (*5*), who used a gold electrode as a reference probe. The initial decrease of the work function is commonly attributed to incorporation of oxygen into the surface, thus building up an inverse surface dipole layer (*6, 7*). The subsequent increase in work function to values higher than the clean metal value can be explained by oxide formation with a concomitant change of the chemical potential. The oxygen pressure dependence of the work function curve may be due to different concentrations of subsurface oxygen. If an oxygen dissolution mechanism is assumed at the initial stages of the reaction, the oxygen concentration near the surface depends on the oxygen uptake from the gas phase and the oxygen diffusion into the bulk; the balance of these processes may therefore be pressure dependent.

In earlier experiments Müller (*5*) found a decrease in the work function below the clean metal value at high oxygen exposures. Such a decrease was not observed in our present experiments. It has to be pointed out, however, that oxidized rare earth surfaces react readily with water vapor, which results in large $\Delta\phi$ drops (see Section 3.2.1). The work function decrease at high oxygen exposures observed by Müller (*5*) may therefore be due to reaction with residual gas water.

A very contrasting behavior as compared to Er is observed for the oxidation of Yb (Fig. 1). The work function change is positive from the very beginning of the oxidation and the overall curve shape does not show a systematic pressure dependence. The relatively small variations observed in Fig. 1 may be caused by different film structures due to slight variations in the evaporation rate.

A different behavior for Er and Yb upon oxidation has also been found by electron spectroscopic techniques. Using XPS, Padalia *et al.* (*8*) have found different uptake kinetics of oxygen on Yb and the other heavy rare earths. The linear uptake observed on Yb was attributed to an island growth mechanism, whereas continuous oxide layer growth was assumed in order to explain the logarithmic uptake on the other heavy rare earths. Bertel *et al.* (*3, 9*) have investigated the plasmon behavior in electron energy loss spectroscopy during oxidation of Er and Yb, and found metal and oxide bulk plasmons to coexist over a wide range of oxygen exposures in the case of

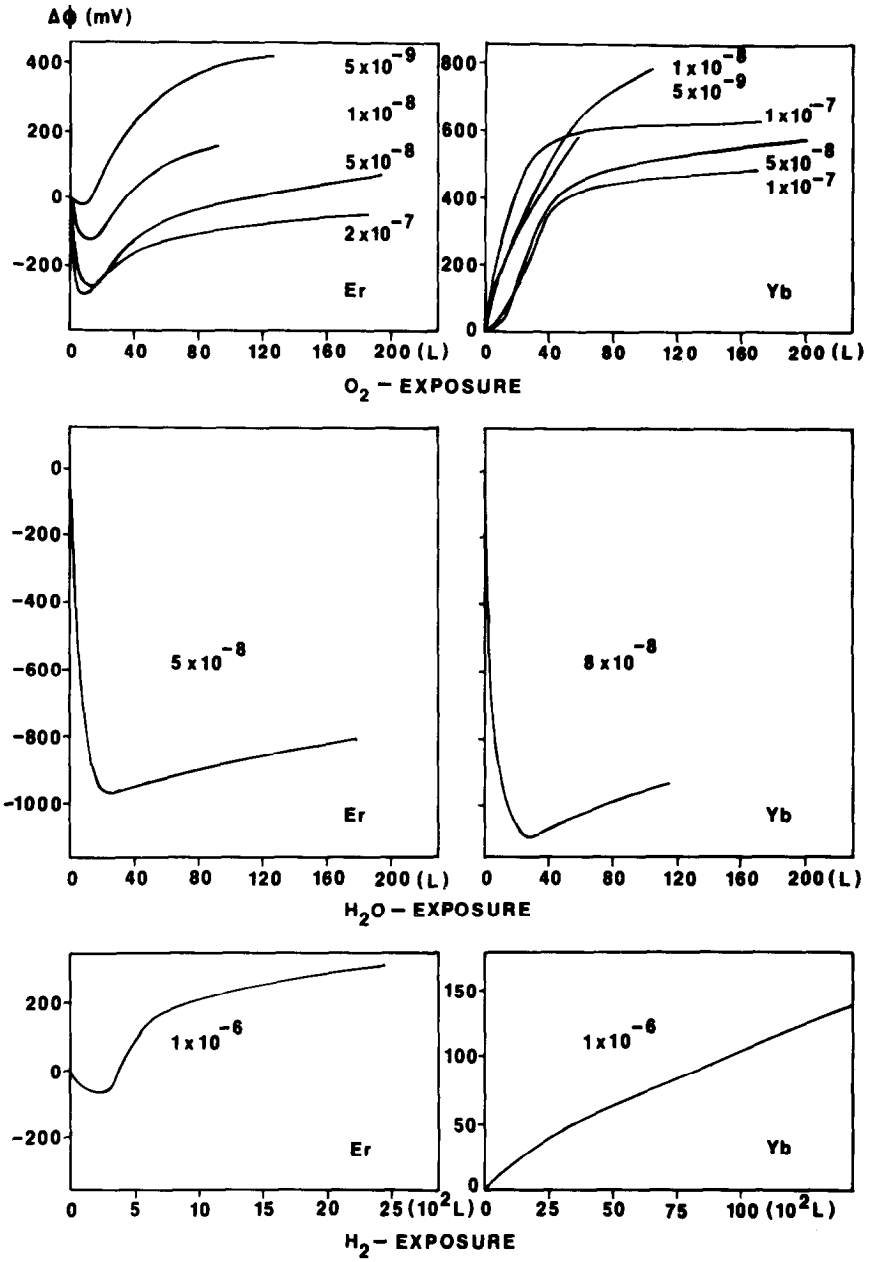

FIG. 1. Work function changes of Er and Yb during reaction with oxygen (top), water (center), and hydrogen (bottom). Numbers beside the work function curves indicate the constant stationary pressure in Torr. Exposures are given in Langmuir (1 L = 1 × 10^{-6} Torr sec).

Yb. Island growth mechanism of the oxide has therefore been inferred for Yb (*3*). The work function results are consistent with that model. The absence of an initial work function decrease in Yb suggests that the oxygen penetration into the metal lattice is slower compared to that in other rare earth metals, thus allowing a surface concentration of oxygen to build up from zero exposure. This initially higher surface concentration of oxygen may then prompt the nucleation of oxide islands.

The observation of reversible effects in $\Delta\phi$ during oxidation yields further support for a distinction between island and uniform layer growth of the oxide phases. Work function changes on Er and Yb surfaces recorded during subsequent exposure and pump-down cycles are shown in Fig. 2. In Er, there is no reversible $\Delta\phi$ change after 3 L O_2 exposure, a very small change after 10 L O_2, but a remarkable reversible work function change of about 100 mV after 40 L O_2. In Yb, similar effects are observed, but the reversible $\Delta\phi$ change is already apparent at 3 L O_2; saturation of the reversible effects is reached after 40 L O_2 with a saturation value of $\sim$100 mV as in the case of Er.

Two explanations may be offered to account for the reversible effects: diffusion of oxygen from near-surface regions into the bulk, and reversible adsorption of oxygen. If diffusion away from the surface were the dominant process, we would expect the work function to move toward its clean metal value once the oxygen pressure is lowered. In the case of Er this would mean a ϕ increase during pumping-down in the region of negative $\Delta\phi$. A work function decrease, however, is always observed here, and we tend to favor an explanation in terms of reversible oxygen adsorption. If we associate, therefore, the reversible $\Delta\phi$ effects with reversible oxygen adsorption on oxidized parts of the rare earth surfaces, the different behavior of Er and Yb can be rationalized in terms of their different oxide growth mechanisms. In the case of Er, oxygen seems to dissolve into near-surface re-

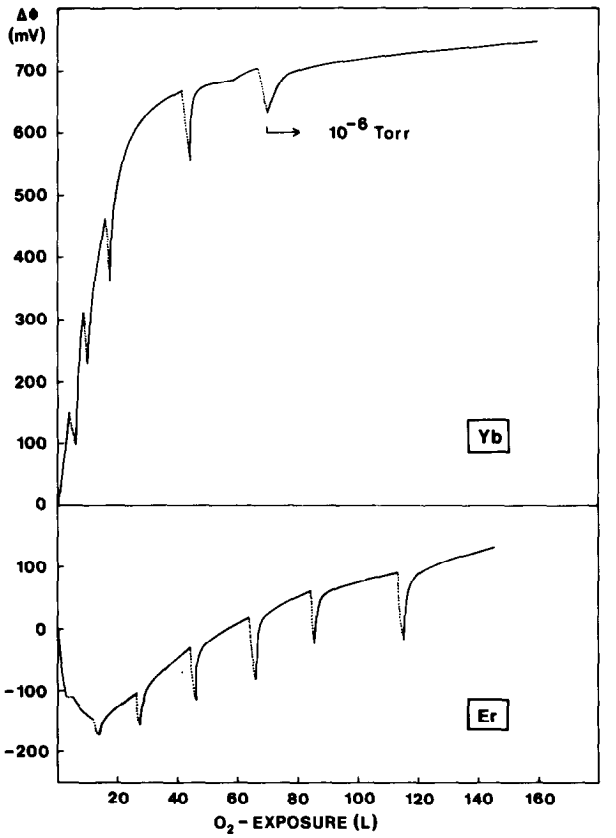

FIG. 2. Demonstration of reversible effects in $\Delta\phi$ during the exposure of Er and Yb to oxygen. The solid lines correspond to an oxygen pressure of 5×10^{-8} Torr, and the dotted lines indicate pumping-down to 3×10^{-9} Torr. The exposure scale has been corrected for the pump-down cycles.

gions during small exposures and hence no reversible effects are observed. Only after further exposure is oxide nucleated and then an increasing amount of reversibly adsorbed oxygen is reflected in corresponding $\Delta\phi$ changes. In Yb, however, oxide islands are nucleated at low exposures and therefore reversible effects can already be observed at these low exposures.

$\Delta\phi$ curves were measured during the reaction of oxygen with Eu and Sm (*10*). As shown in Fig. 3, the general pattern of the results on Eu and Sm is similar to that on Er, i.e., an initial decrease of ϕ is followed by an increase to values higher than the clean metals; the depth and the position of the work function minimum are systematically dependent of oxygen pressure. The data on Eu and Sm are therefore consistent with an oxygen dissolution model at the initial stages of the oxidation, as has been inferred for the heavier rare earth metals (*2*).

3.1.2. Oxidation of rare earth metals by water. The work function changes of Er and Yb metal film surfaces exposed to water at pressures of 5.10^{-8} and 8.10^{-8} Torr, respectively, are shown in the center of Fig. 1. A sharp decrease of ~1000 mV in both cases is followed by a slower increase. The $\Delta\phi$ curves are pressure independent and no reversible effects are observed.

X-Ray diffraction studies of the reaction of rare earth metal thin films with water have indicated hydride, oxyhydride, and oxide phases as reaction products (*11–13*). In Er, no reaction at all could be detected at room temperature by X-ray diffraction, whereas at elevated temperatures Dy and

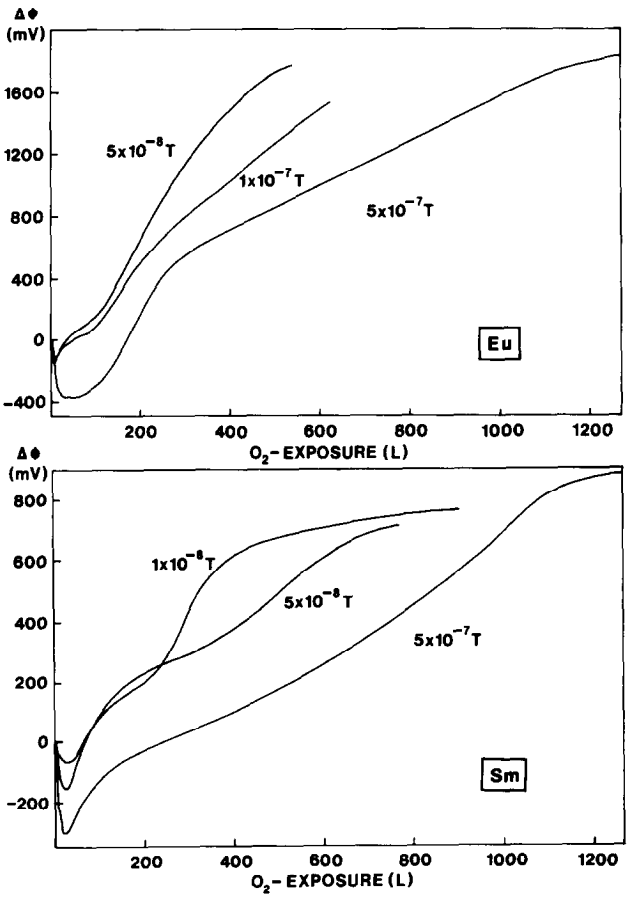

FIG. 3. Work function changes of Eu and Sm during oxygen exposure.

Gd were reported to be completely converted into the corresponding dihydrides with no signs of oxide formation (*11*). In contrast, Smith *et al.* (*14*) proved by Auger spectroscopy that large amounts of oxygen are incorporated into the bulk under the above reaction conditions. The absence of oxide X-ray diffraction lines reported previously (*11*) is presumably due to the formation of amorphous oxide phases or to oxygen dissolution. Netzer *et al.* (*15*) and Padalia *et al.* (*8*) have used UPS and XPS, respectively, to show that the interaction of water with heavy rare earth metals results in water splitting and OH group formation at the surface. The large decrease in work function reported here can therefore be attributed to the buildup of an OH surface layer. Adopting a value of $\Delta\phi = -1000$ mV and assuming 10^{15} OH groups per square centimeter, the surface dipole moment per OH entity is ~25% of the OH dipole moment in water. This seems to be a reasonable value for adsorbed OH and supports the assumption of water dissociation on rare earth metal surfaces.

The $\Delta\phi$ measurements suggest the same H_2O uptake mechanism on both Er and Yb. In contrast, the uptake curves derived from the O 1*s* intensity in XPS are quite different for Er and Yb (*8*). An oxide island growth mechanism with OH groups on top of the islands has been proposed, possibly with the concomitant formation of a dihydride phase, but a hydroxide or oxyhydroxide phase cannot be excluded either (*2*).

3.1.3. Hydrogenation of rare earth metals. Work function changes of Er and

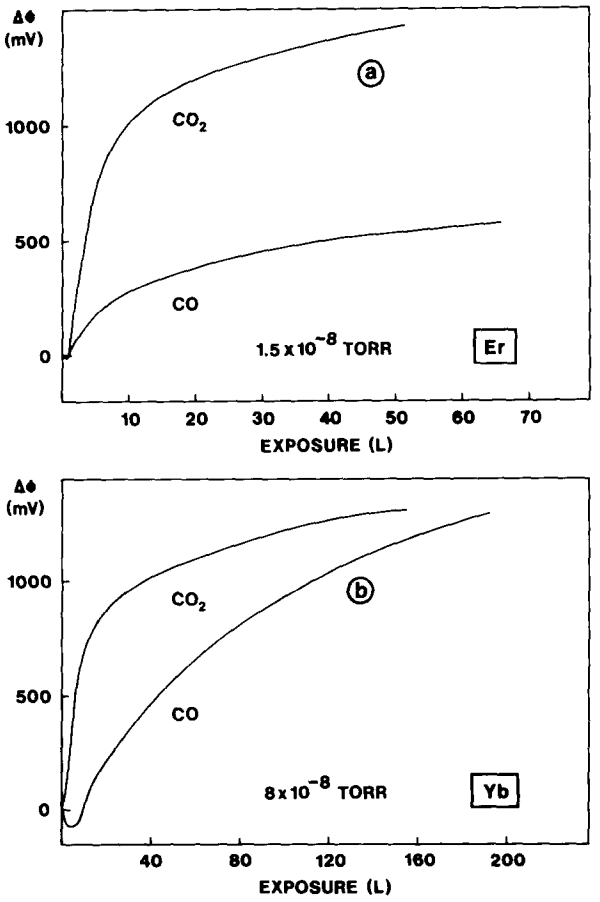

FIG. 4. Work function curves of Er (a) and Yb (b) exposed to CO and CO_2.

Yb metal film surfaces exposed to hydrogen at 10^{-6} Torr are shown in the bottom panels of Fig. 1. The initial work function decrease of ~40 mV in Er seems to be pressure independent, as it was also observed by Müller and Surplice (*16*) at 10^{-4} Torr H_2 partial pressure. The subsequent work function increase is quite slow, and saturation is not reached up to exposures as high as 2500 L for Er and 14,000 L for Yb.

It is tempting to associate the initial work function decrease with OH group formation due to oxygen contamination of the evaporated Er films. However, no correlation was found between the magnitude of the work function decrease and the contaminant oxygen Auger signal. Müller and Surplice (*16*) have associated the work function decrease with incorporation of $H^{-\delta}$ ($\delta < 1$) species into the surface and the subsequent increase with the occupation of adsorption sites on top of the surface layer. The continuous increase of the work function and the absence of saturation at quite large H_2 exposures is obviously caused by hydrogen diffusion and incorporation into the bulk.

In Yb, the hydrogen uptake seems to be much slower than in Er. This could be associated with the divalency of Yb metal. Some indication for such behavior may be found in the work of Atkinson *et al.* (*17*), who observed the initial sticking probability of H_2 on Sm to be 2 orders of magnitude

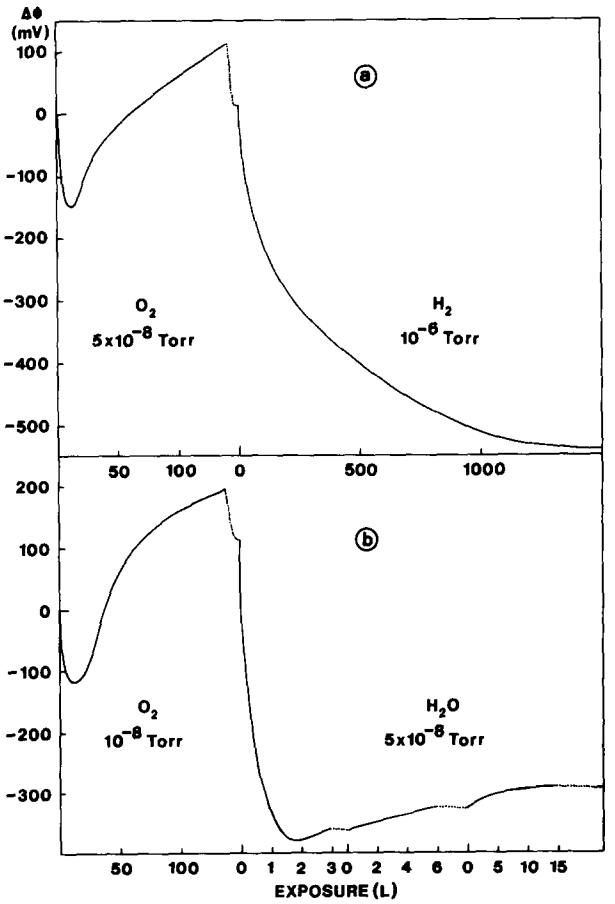

FIG. 5. $\Delta\phi$ of reactions on oxidized Er: (a) exposure to 5×10^{-8} Torr oxygen is followed by 1×10^{-6} Torr H_2; (b) exposure to 1×10^{-8} Torr O_2 is followed by 5×10^{-8} Torr H_2O.

lower than that on other trivalent rare earth metals. As divalency at the surface of Sm metal has meanwhile been established (*18, 19*), it is tempting to associate the low reactivity of Sm toward H_2 with divalent surface character. The present results on Yb are consistent with that interpretation, and very recent experiments of H_2 uptake on divalent Eu in this laboratory (*20*) confirm the relatively low reactivity of divalent rare earth metals toward hydrogen.

3.1.4. Interaction of rare earth metals with CO and CO_2. In Fig. 4 the work function curves of Er and Yb surfaces exposed to CO and CO_2 are displayed. On Er a small initial decrease ($\Delta\phi \simeq -10$ mV) is followed by a large increase for both CO and CO_2. After exposure to 120 L CO the work function increases by ~1000 mV (not shown in Fig. 4), whereas a value of $\Delta\phi = +1200$ mV is reached after only 20 L CO_2. A very similar behavior is observed on Yb/CO and Yb/CO_2; the only difference is a slightly larger initial decrease ($\Delta\phi \simeq -70$ mV) upon exposure to CO and the absence of the initial decrease upon exposure to CO_2. The work function curves for Er/CO in Fig. 4a are similar to those reported by Surplice and Brearley (*21*).

High-resolution Auger spectra of CO and CO_2 on Er and Yb suggest dissociative adsorption for both adsorbates: the typical molecular lineshapes of oxygen and carbon Auger transitions (*22*) are not observed; instead, "carbidic-like" (C KVV) and "oxide-like" (O KVV) lineshapes are obtained (*23*). Furthermore, the similar Auger lineshapes for CO and CO_2 and the similar C/O intensity ratios indicate similar surface complexes for both adsorbates (*23*). The large work function changes reported in this work are consistent with dissociative adsorption of CO and CO_2 on rare earth metal surfaces. Predominantly dissociative adsorption of CO on Sc has also been inferred recently from XPS data by Affrossman (*24*). He suggested the formation of a ternary carbide–oxygen compound, but further work is needed to specify the detailed nature of these structures.

3.2. Reactions on Oxidized Rare Earth Surfaces

In this and the following section experiments are described where rare earth metal films were allowed to react with one reactant before being exposed to a second reactant. Work function changes were monitored during the course of these reactions.

Figure 5a shows work function changes of an Er surface, which is exposed first to oxygen (5×10^{-8} Torr) up to saturation and then to hydrogen (10^{-6} Torr). Interaction of H_2 with an oxidized Er surface leads to a work function decrease of 300–500 mV, the exact value depending on the preoxidation conditions. A similar work function decrease is observed on oxidized Yb upon exposure to H_2. These work function changes are not only much larger than those detected upon simple reaction of H_2 with the metals, but also of the opposite sign. We propose dissociative adsorption of H_2 on the oxidized surfaces and the formation of OH groups on top of the oxides.

Based on UPS evidence formation of OH groups on oxidized Er by reaction with H_2 at room temperature has been reported previously by Netzer *et al.* (*15*). Additional support for this model is obtained here by comparison with $\Delta\phi$ measurements of H_2O interaction with oxidized Er or Yb, where OH group formation is well established in the catalytic literature (*25*). In Fig. 5b the Er surface has been saturated with O_2 at 1×10^{-8} Torr and then exposed to 5×10^{-8} Torr H_2O. Exposure of H_2O causes a work function decrease of ~500 mV relative to the oxidized surface in remarkable agreement with the H_2 reaction experiments (Fig. 5a). The rate of the work function change in the two cases, however, is rather different. For H_2 ~1000 L are necessary to produce the maximum work function drop, whereas only ~2 L of H_2O exposure are needed. This indicates that H_2 dissociation is the rate-limiting step in the reaction of H_2 with the oxidized surface. In Fig. 5b, the

work function increases slightly after the minimum during further H_2O exposure, but no reversible effects are observed. The slight increase may be due to changes in the underlying oxide structure or to the formation of hydroxide phases.

If the reaction of H_2 with the oxidized rare earth surfaces has come to equilibrium, i.e., the work function has reached a stationary value, subsequent exposure to H_2O produces no significant work function change. If, on the other hand, the reaction of H_2 is stopped before completion, subsequent reaction with H_2O is evidenced by a further work function drop. Both reactions seem to be therefore competitive processes, which eventually lead to a fully hydroxylated surface layer of the oxides.

Reaction with hydrogen can still occur on hydroxylated rare earth surfaces. This is demonstrated in experiments where clean rare earth metal films (Er, Yb) were oxidized with H_2O and then exposed to hydrogen. An increase in work function is observed; the magnitude and the rate of change on Er/H_2O are very similar to that on Er metal, but the rate on Yb/H_2O is much faster than that on Yb metal. It appears, therefore, that there are still enough active sites for H_2 dissociation on OH-covered film surfaces. The increase of the H_2 reaction rate on Yb/H_2O as compared to on Yb metal may be due to the different valency of Yb atoms in the two systems. Yb is divalent in the metal and it is trivalent in the oxide (*3*). As the sticking probability of H_2 seems to be low on divalent rare earth metals (see Section 3.1.3), the acceleration of H_2 uptake on the trivalent Yb/H_2O system suggests that the presence of trivalent metal cations may be crucial for hydrogen dissociation.

Finally, we would like to mention that experiments to detect CO adsorption on oxidized rare earth film surfaces at room temperature proved to be unsuccessful. Both Auger spectroscopy and $\Delta\phi$ measurements gave negative results. Under present pressure and temperature conditions ($<10^{-6}$ Torr CO, room temperature) CO seems to be unreactive toward rare earth oxide surfaces.

3.3. Reactions on Partially Hydrided Rare Earth Surfaces

Exposing a partially hydrided Er film to O_2 results in a small work function increase followed by a decrease, which seems to be linear with O_2 exposure. Subsequent exposure to H_2O causes a further work function decrease. This reaction sequence is shown in Fig. 6a. In Fig. 6b the Er film is dosed with H_2O after H_2 exposure. Here, the work function is lowered by ~900 mV after H_2O exposure to a hydrogen-covered surface. This is similar to what is observed upon H_2O exposure of a clean or an oxidized surface (cf. Figs. 1 and 5b), but the reaction rate seems to be fastest on the oxidized surface.

The negative work function changes in both experiments suggest formation of surface hydroxyl groups. The initial work function increase during O_2 exposure may be due to on-top adsorption of oxygen atoms, which is then gradually replaced by OH formation. Accordingly, the admission of H_2O after extensive O_2 treatment of the hydrided Er film has little effect on $\Delta\phi$, because the surface is already hydroxylated. Formation of surface OH by H_2O interaction on hydrided films is slower than on oxidized films, but occurs at a comparable rate as on clean metal films (cf. Fig. 1, center panels).

4. CONCLUSIONS

Work function measurements on rare earth surfaces can provide valuable complementary information on surface reactions, in particular if employed in conjunction with other surface sensitive methods such as Auger or photoelectron spectroscopy. In this paper we report $\Delta\phi$ measurements on evaporated rare earth films performed under clean ultrahigh vacuum conditions:

Rare earth metal surfaces are shown to

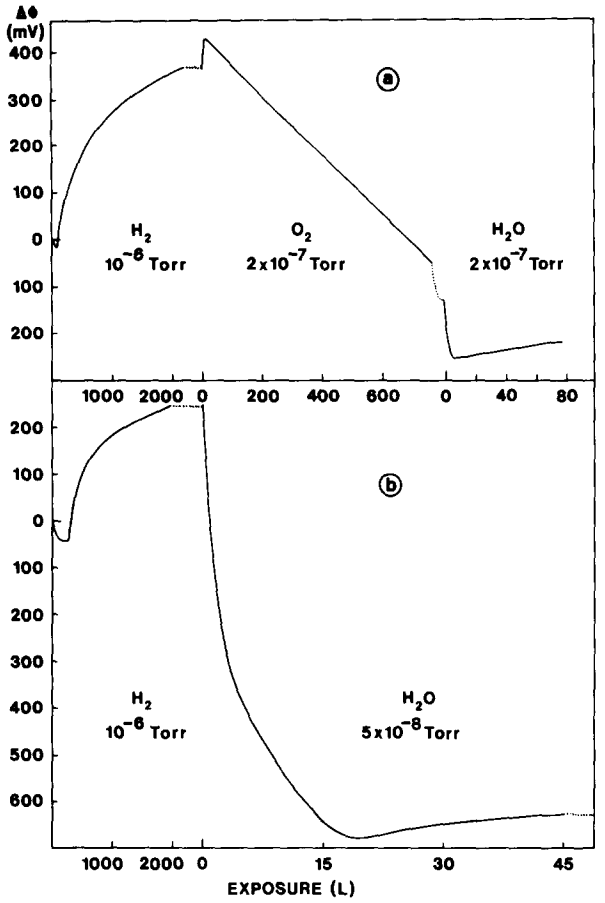

FIG. 6. $\Delta\phi$ of reactions on partially hydrided Er: (a) exposure to 1×10^{-6} Torr H_2 is followed by 2×10^{-7} Torr O_2, and then by 2×10^{-7} Torr H_2O; (b) exposure to 1×10^{-6} Torr H_2 is followed by 5×10^{-8} Torr H_2O.

react readily with O_2, H_2, H_2O, CO, and CO_2. On Yb, $\Delta\phi$ measurements during oxidation are consistent with an island growth mechanism at the initial stages of the oxidation process. This is in contrast to other rare earths, where oxygen dissolution with subsequent continuous oxide overlayer formation is indicated. The reaction with H_2O produces very similar work function changes on Yb and Er, which are attributed to surface OH formation. The reactivity of divalent Yb metal toward H_2 seems to be much lower than that of trivalent Er. The present work function data are consistent with dissociative adsorption of CO and CO_2 on rare earth metals.

Dynamic work function measurements of consecutive reactions on rare earth surfaces are presented and discussed. The formation of surface hydroxyl species on oxidized and hydrided rare earth metal surfaces by room temperature reaction with H_2, H_2O, or O_2, respectively, is substantiated by our $\Delta\phi$ data, but different reactivities on oxidized and hydrided surfaces are noted.

ACKNOWLEDGMENTS

This work was supported by the Fonds zur Förderung der Wissenschaftlichen Forschung of Austria and the Austrian Nationalbank. We are grateful to J. A. D. Matthew, University of York, England, and to P. R. Norton, Chalk River Nuclear Laboratories, Canada, for valuable discussions.

REFERENCES

1. Rosynek, M. P., *Catal. Rev. Sci. Eng.* **16,** 111 (1977).
2. Netzer, F. P., and Bertel, E., "Handbook on the Physics and Chemistry of Rare Earths" (K. A. Gschneider and L. Eyring, Eds.), Vol. 5, Chap. 3. North-Holland, Amsterdam, 1983.
3. Bertel, E., Strasser, G., Netzer, F. P., and Matthew, J. A. D., *Surf. Sci.* **118,** 387 (1982).
4. Engelhardt, H. A., Feulner, P., Pfnür, H., and Menzel, D., *J. Phys. E Sci. Instrum.* **10,** 1133 (1977).
5. Müller, J., *Surf. Sci.* **69,** 708 (1977).
6. Hofmann, P., Wyrobisch, W., and Bradshaw, A. M., *Surf. Sci.* **80,** 344 (1979).
7. Michel, R., Gastaldi, J., Allasia, C., and Jourdan, C., *Surf. Sci.* **95,** 309 (1980).
8. Padalia, B. D., Gimzewski, J. K., Affrossman, S., Lang, W. C., Watson, L. M., and Fabian, D. J., *Surf. Sci.* **61,** 468 (1976).
9. Bertel, E., Netzer, F. P., and Matthew, J. A. D., *Surf. Sci.* **103,** 1 (1981).
10. Strasser, G., Ph.D. thesis, University of Innsbruck, 1983.
11. Dexpert-Ghys, J., Loier, C., La Blanchetais, C. H., and Caro, P. E., *J. Less-Common Met.* **41,** 105 (1975).
12. Holloway, D. M., and Swartz, W. E., *Appl. Spectrosc.* **31,** 167 (1977).
13. Oesterreicher, H., Bittner, H., and Shuler, K., *J. Solid State Chem.* **29,** 191 (1979).
14. Smith, H. K., Moldovan, A. G., Craig, R. S., Wallace, W. E., and Gankar, S. G., *J. Solid State Chem.* **32,** 239 (1980).
15. Netzer, F. P., Wille, R. A., and Grunze, M., *Surf. Sci.* **102,** 75 (1981).
16. Müller, J., and Surplice, N. A., *J. Phys. D* **10,** 213 (1977).
17. Atkinson, G., Coldrick, S., Murphy, J. P., and Taylor, N., *J. Less-Common Met.* **49,** 439 (1976).
18. Wertheim, G. K., and Crecelius, G., *Phys. Rev. Lett.* **40,** 813 (1978).
19. Bertel, E., Strasser, G., Netzer, F. P., and Matthew, J. A. D., *Phys. Rev. B* **25,** 3374 (1982).
20. Strasser, G., and Netzer, F. P., unpublished results.
21. Surplice, N. A., and Brearley, W., *Surf. Sci.* **72,** 84 (1978).
22. Netzer, F. P., *Appl. Surf. Sci.* **7,** 289 (1981).
23. Netzer, F. P., and Bertel, E., unpublished results.
24. Affrossman, S., *Surf. Sci.* **111,** 1 (1981).
25. See, e.g., Ref. (2) and references cited therein.